PERGAMON

Aerosol Science 32 (2001) 33–48

Journal of
Aerosol Science

www.elsevier.com/locate/jaerosci

Field tests of a passive aerosol sampler

Jeff Wagner*, David Leith

Department of Environmental Sciences and Engineering, University of North Carolina, CB # 7400, Rosenau Hall, Chapel Hill, NC 27599, USA

Received 8 February 2000; received in revised form 25 April 2000; accepted 26 April 2000

Abstract

Field tests have been conducted to evaluate the passive aerosol sampler described by Wagner and Leith (2000a,b) *Aerosol Science Technology*, in press). Tests were conducted in a well-ventilated occupational environment with coarse, high-concentration aerosols. Measured friction velocities were less than $0.4\,m\,s^{-1}$, a range in which passive sampler performance does not depend on turbulence. Passive sampler results correlated well with those of eight-stage cascade impactors, with $R^2 = 0.80$ and 0.93 for PM2.5 and PM10, respectively. Average disagreement between the passive samplers and the impactors was -31 and 41% for PM2.5 and PM10, respectively. These discrepancies were attributed to the small amount of fine particles present, hygroscopic particles, and particle bounce in the impactors. The average CV_{PM10} for all samples was 20%. The average $CV_{PM2.5}$ for non-hygroscopic samples was 16%. The average $CV_{PM2.5}$ for hygroscopic samples was much higher, 59%; water losses in these samples created ill-defined particle boundaries which led to imprecision.

Keywords: Aerosol sampling; Passive sampling; Sampler comparisons

1. Introduction

Many techniques for characterizing aerosols are relatively obtrusive, expensive, maintenance-intensive, and costly. These qualities stem from the air-moving and/or detection components housed within most samplers. In contrast, the aerosol sampler described by Wagner and Leith (2000a,b) is of a simple, passive design; after sampling, the collected particles are analyzed by microscopy. The passive sampler can sample unattended for hours to weeks and has potential utility as a personal sampler. It is small, lightweight (1.7 g), inexpensive, and easy to operate.

* Corresponding author. Tel.: 1-919-966-7337; fax: 1-919-966-7911.
E-mail address: jwagner@email.unc.edu (J. Wagner).

0021-8502/00/$ - see front matter
PII: S0021-8502(00)00055-0

Nomenclature

C	bulk aerosol concentration at infinite distance from surface
C_c	Cunningham correction factor
D	Brownian diffusion coefficient
d_a	aerodynamic diameter
$dC/d \log d_a$	concentration normalized by width of size bin
d_{ev}	equivalent-volume diameter
d_{pa}	projected-area diameter
F	flux of particles to a surface
g	gravitational acceleration constant
I	$=(I^+/u_*)$
I^+	term defined by Eq. (3)
n	frequency of turbulent fluctuations
p	probability observed relationship occurred by chance
R^2	correlation coefficient
Re_p	particle Reynolds number $=(d_a v_t/v)$
Sc	Schmidt number ($=v/D$)
S_d	dynamic shape factor
S_v	volume shape factor
T	turbulence intensity
t	time
$u(t)$	wind speed at time t
u_*	turbulent friction velocity
$u'(t)$	fluctuating component of wind velocity at time t
v_{amb}	ambient deposition velocity
v_{dep}	overall deposition velocity
v_t	terminal settling velocity

Greek letters

γ_m	mesh factor
v	kinematic viscosity
ρ_0	unit particle density
ρ_p	particle density
τ	particle relaxation time
τ^+	$=(\tau u_*^2/v)$

In the passive sampler, particles travel through a protective, stainless-steel mesh (Fig. 1) and deposit on a smooth collection surface by gravity, inertia, and diffusion. Afterwards, the sampler is sealed in a case and transported to the lab for analysis. Depending on one's needs and capabilities, various microscopy types can be used. Scanning electron microscopy (SEM)

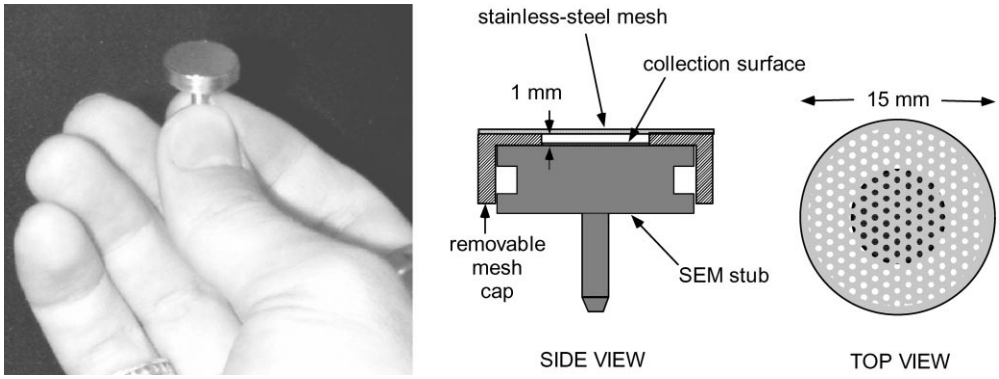

Fig. 1. Passive aerosol sampler.

with energy-dispersive X-ray fluorescence (EDXRF) is a convenient choice. During SEM/EDXRF analysis, collected particles larger than 0.1 μm are representatively counted and sized, and chemical constituents can be determined. The mass flux to the sampler is obtained as a function of aerodynamic diameter using the microscopy data in conjunction with particle shape and density factors.

The flux and a deposition velocity model are then used to estimate the average mass concentration and size distribution over the sampling period

$$C = \frac{F}{v_{\mathrm{dep}}} = \frac{F}{v_{\mathrm{amb}}\,\gamma_{\mathrm{m}}}, \tag{1}$$

where C is the average mass concentration over the sampling period and F is the mass flux (particles collected/(area-time)) determined from the microscopy, v_{dep} is the particle deposition velocity and is comprised of a theoretical component, v_{amb}, and an empirical mesh factor, γ_{m}, as described previously (Wagner & Leith, 2000a). All terms are calculated as a function of aerodynamic diameter, d_{a}. The size distribution information can then be used to determine PM2.5, PM10, respirable, inhalable, or any other size-dependent concentration of interest.

v_{amb} represents the ambient particle deposition rate to a flat plate, and has been derived using gravitational, inertial, and diffusive mechanisms (Wagner & Leith, 2000a)

$$v_{\mathrm{amb}} = \frac{-v_t}{[(1 - 0.67\tau^{0.49}u_*^{-0.02}\nu^{-0.49}v_t)\mathrm{e}^{-v_t I}] - 1}, \tag{2}$$

where v_t $(= \tau g)$ is the terminal settling velocity, τ is the particle relaxation time, g is the acceleration due to gravity, u_* is the friction velocity, ν is the kinematic viscosity, $I = (I^+/u_*)$, and

$$I^+ = \frac{1}{\dfrac{3\sqrt{3}}{29\pi}\,\mathrm{Sc}^{-2/3} + 6.2\times 10^{-4}(\tau^+)^2} \tag{3}$$

has been adapted from the work of Wood (1981), where Sc is the Schmidt number and $\tau^+ = (\tau u_*^2/\nu)$. When, $u_* < 0.4\ \mathrm{m\ s^{-1}}$, corresponding to a relatively low-turbulence environment, Eq. (2) can be

greatly simplified

$$v_{amb} \cong v_t. \tag{4}$$

This condition should be met in most indoor and some outdoor environments.

The empirical portion of the deposition velocity, γ_m, accounts for the effects of the mesh cap on the deposition rate and was determined in wind tunnel tests (Wagner & Leith, 2000b)

$$\gamma_m = 1, \qquad d_a < 1.63\ \mu m,$$
$$\gamma_m = (5.95 \times 10^{-3})Re_p^{-0.439}, \qquad d_a \geqslant 1.63\ \mu m, \tag{5}$$

where $Re_p = (d_a v_t/v)$.

The passive aerosol sampler tested here is similar in concept to those of other investigators, but possesses several important differences as well. The passive dust monitor of Brown, Hemingway, Wake, and Thompson (1995) collects particles electrostatically with a charged electret and can be analyzed gravimetrically. Thus far, the electrical mobility data required for a priori calculations have proved difficult to obtain. Correlations with conventional samplers have had some success, but have been hampered by electret charge loss and small sample size (Thorpe, Hemingway, & Brown 1999). The passive sampler of Vinzents (1996) utilizes collection mechanisms similar to the sampler of this work, but can be analyzed using total light extinction and has a larger and heavier design. Both investigators have emphasized total concentration measurements; in contrast, the intent of the sampler of this work is to measure concentration as a function of particle size.

This paper describes the results of the first field tests of the passive aerosol sampler shown in Fig. 1. The objectives of these tests were to determine the sampler's performance under real-world turbulence and aerosol conditions. To this end, agreement with impactor PM2.5 and PM10 measurements was determined, and precision was assessed using collocated passive samplers. In addition, turbulence was measured to investigate the applicability of Eq. (4).

2. Methods

2.1. Test site

Field tests were conducted at a glass manufacturing plant. Two plant locations with unusually high aerosol concentrations were chosen to minimize sampling times. Location 1 was inside a garage-like enclosure where railroad cars unloaded large quantities of dusty materials into hoppers. These materials were then transferred via conveyer belt to the tops of several large storage silos. Location 2 was situated at the point where the materials dropped from the conveyer belt into the silos. At both locations, the unloading of the materials into confined spaces caused them to aerosolize.

2.2. Sampling methods

Five sampling events were recorded, each utilizing three passive samplers collocated with one eight-stage, 1 cfm Andersen impactor (Andersen Instruments Inc., Smyrna, GA). The sampling setup used for each sampling event is shown in Fig. 2. The impactor stages were equipped with oleic acid-coated polycarbonate membrane filters (Isopore, Millipore, Bedford, MA) to minimize

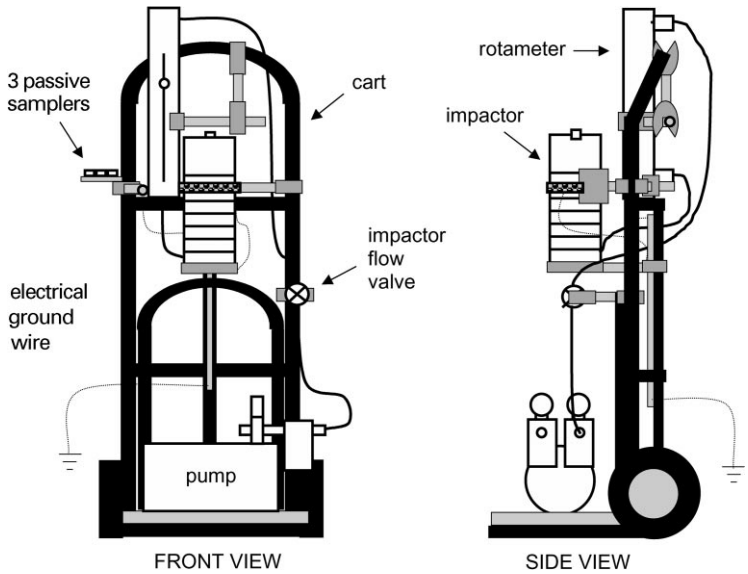

Fig. 2. Experimental apparatus for field tests.

Table 1
Environmental conditions

Sampling event	Location	Sample time (min)	Temperature (C)	RH (%)	Typical wind speeds ($m\ s^{-1}$)
1	1	473	21	57	0.3
2	2	183	21	58	0.1
3	2	250	21	58	0.1
4	2	32	18	62	0.1
5	2	27	18	62	0.3

particle bounce. This technique was adapted from methods described by Turner and Hering (1987). The passive samplers were prepared and transported following the method of Wagner and Leith (2000b). Both the passive samplers and the impactor were electrically grounded.

Sampling times ranged from approximately 0.5–8 h and are listed in Table 1. Ambient temperatures and relative humidities were recorded during sampling with a digital hygrometer (Fisher Scientific, Pittsburgh, PA). Qualitative mass concentrations and wind speeds were monitored real-time using an aerosol photometer (DustTRAK, TSI, Inc., St. Paul, MN) and anemometer (Velocicheck Model 8830, TSI, Inc., St. Paul, MN).

2.3. Turbulence measurement

Turbulence was characterized at Location 1 by taking several measurements near the sampling setup. During the first set of measurements, the enclosure doors were open to the outdoors, and

thus a source of cross-ventilation. The next morning, measurements were taken with the railroad cars substantially blocking the doors and reducing ventilation. Turbulence was measured using an anemometer controller/signal processor (IFA-100 Intelligent Flow Analyzer, TSI Inc., St. Paul, MN), a disposable hot-film anemometer probe (Model 1201-20, TSI Inc., St. Paul, MN), a portable oscilloscope (TDS-210, Tektronix, Wilsonville, OR), and acquisition software (WaveStar, Tektronix, Wilsonville, OR) run on a laptop PC. This measurement system was capable of recording velocity traces for 45 s with 50 data points per second. Thus, this system was sensitive enough to capture relatively high-frequency velocity fluctuations, but was also suited to a busy industrial environment.

The anemometer system was calibrated in the laboratory prior to the field tests. A rectangular wind tunnel with a 48 cm × 50 cm cross-section, flanged entrance, and orifice meter was used for the calibration. The IFA-100's signal processor was used to subtract a constant voltage level from the transducer output, and the remaining voltage was then multiplied and sent to the oscilloscope. There, a large negative voltage offset was applied, and the "volts/div" control was increased until the fluctuations approached full scale. The resulting oscilloscope signal could typically be read to within 2% of the magnitude of the velocity fluctuations.

For each velocity trace, the turbulence intensity, T, was calculated

$$T = \frac{\sqrt{\overline{u'(t)^2}}}{\bar{u}} \frac{\sqrt{\overline{(u(t) - \bar{u})^2}}}{\bar{u}}, \tag{6}$$

where $u(t)$ is the measured velocity at time t, $u'(t)$ is the fluctuating component of the velocity, and the bars represent averages over the measurement period (Schlichting, 1979). The friction velocity could then be calculated using the empirical relationship (Hughmark, 1977; Schneider, Bohgard, & Gudmundsson, 1994)

$$u_* = \frac{\sqrt{\overline{u'(t)^2}}}{0.63} = \frac{\bar{u}T}{0.63}. \tag{7}$$

2.4. Sample analysis

Impactor concentrations were obtained gravimetrically with an analytical balance (Mettler Toledo Model AE200, Toledo, OH) interfaced to a laptop PC. Pre-weighing was conducted at least 1 h after applying oleic acid to the impactor substrates. The balance was located in a room in the plant with relatively clean and stable environmental conditions. Replicate stage weights were recorded before and after sampling, and four of the five impactor samples were weighed a third time after an additional 24 h to insure that the aerosol was at equilibrium.

Two blank impactor stages were prepared with polycarbonate filters and oleic acid, placed inside blank impactors, and weighed in conjunction with each impactor analysis. In addition, one passive sampler blank was associated with each sampling event. This blank was prepared simultaneously with the three passive samplers, but was left inside the protective case during the sampling period. The blank accounted for any contamination that may have occurred during sampler preparation, transport back to the lab, or handling during analysis. The results of both the impactors and passive samplers were corrected by subtracting their respective blank values.

Passive samplers were analyzed with SEM and qualitative XRDF using procedures described by Wagner and Leith (2000a,b). All size distributions were divided into the same nine arbitrary size bins between 0.1 and 10 μm. Eq. (4) was assumed to be valid for these tests. The following shape factors were used to perform equivalent diameter and mass conversions (Davies, 1979; Noll, Fang, & Watkins, 1988)

$$S_v = d_{pa}/d_{ev}, \tag{8}$$

$$S_d = \frac{\rho_p C_{c,dev}}{\rho_0 C_{c,da}} \left(\frac{d_{dev}}{d_a} \right)^2, \tag{9}$$

where S_v is the volume shape factor, S_d is the dynamic shape factor, d_{pa} is the projected area diameter, d_{ev} is the equivalent-volume diameter, C_c is the Cunningham slip correction factor, and d_a is the aerodynamic diameter.

Representative shape factors and densities were determined for each sample as follows: first, values were assumed for each compound present in the samples (Table 2). Densities for all compounds and shape factors for sand were found in the literature (Wagner & Leith, 2000a; CRC Handbook of chemistry and Physics, 1997). Shape factors for dolomite, soda ash, and lime were estimated by comparing their SEM-observed shapes to those of particles that appear in the Particle Atlas (McCrone & Delly, 1973a,b) and that have published shape factors (Wagner & Leith, 2000a). Dolomite had a similar shape as sand and was assigned the same shape factors. Soda ash and lime were both non-flaky and compact, and thus were assigned shape factors in the range corresponding to quartz, bituminous coal, gypsum, and limestone. The range of shape factors for these particles is only $\pm 15\%$ about their mean. Next, the composition of each sample was estimated on a mass-fraction basis using (a) the identities of the aerosolized materials, provided by plant workers, (b) the knowledge that only one type of aerosol was generated at a time, (c) mass concentrations estimated by the DustTRAK and impactor, and (d) the approximate fraction of sampling time that each material was aerosolized. Then, mass-weighted averages of the parameters in Table 2 were performed to obtain the representative parameters for each sample (Table 3). Because the aerosol species were known and measurements were available to directly estimate mass fractions, this experiment was a relatively ideal case. In circumstances where neither type of information is available, aerosol composition must be determined from the analysis procedure. When using SEM, this information can be obtained with semi-quantitative EDXRF.

Neither the passive sampler nor the impactor had size bins with upper size limits equal to 2.5 μm. For each sample, linear interpolation was performed on the size bin containing 2.5 μm to determine the fraction of the bin's mass that was less than 2.5 μm. This fraction was then added to the sum of

Table 2
Assumed particle shape factors and densities

Aerosol	Volume shape factor S_v	Dynamic shape factor S_d	Particle density (g cm^{-3})
Sand	1.3	1.6	2.50
$CaMg(CO_3)_2$	1.3	1.6	2.86
Na_2CO_3	1.4	1.4	2.54
CaO	1.4	1.4	3.34

the smaller size bins to determine PM2.5. Because the upper limits of the passive samplers' largest size bins were not exactly 10 μm, a similar procedure was used to determine PM10.

3. Results

Temperatures, relative humidities (RH), and wind speeds measured during the field tests are presented in Table 1. In general, temperature and RH were moderate and wind speeds were low. All sampling events involved high-concentration, coarse aerosols. Impactor PM10 concentrations ranged between 0.8 and 36 mg m^{-3}, and the fraction of PM10 mass with $d_a > 2.5$ μm ranged from 83 to 93%. Most particles collected by the passive samplers were in the coarse range as well, with an average of 15 counts per sampler for particles with $d_a < 2.5$ μm and 177 counts per sampler with $d_a < 10$ μm (Table 4). The majority of each sample was composed of either soda ash (Na_2CO_3) or

Table 3
Representative particle shape factors and densities for sampling events

Sampling event	Estimated composition by mass	Avg. volume shape factor S_v	Avg. dynamic shape factor S_d	Avg. particle density (g cm^{-3})
1	59% Na_2CO_3 34% $CaMg(CO_3)_2$ 7% sand	1.36	1.48	2.64
2	84% Na_2CO_3 16% sand	1.38	1.43	2.53
3	88% Na_2CO_3 12% sand	1.39	1.42	2.54
4	98% CaO 2% sand	1.40	1.40	3.33
5	99% CaO 1% sand	1.40	1.40	3.33

Table 4
Analysis characteristics

Sampling event	Avg. counts per passive sampler		Impactor	
	PM2.5	PM10	PM10 (mg m^{-3})	PM10–PM2.5 PM10
1	5.8	66.3	0.81	0.93
2	12.3	212	11.8	0.90
3	35.3	416	11.3	0.90
4	13.6	87.3	17.9	0.83
5	9.9	104	36.4	0.86
Average	15.4	177	15.6	0.88

lime (CaO), with the residual amount consisting of dolomite ($CaMg(CO_3)_2$) and/or sand (predominantly SiO_2) (Table 3). All passive sampler blanks showed relatively low levels of contamination, with an average ratio of (blank PM10/sample PM10) of 5.6%.

Fig. 3 shows a typical velocity trace used to calculate friction velocities. Fig. 4 shows two sets of measured friction velocities over time. The average friction velocities for the two conditions were

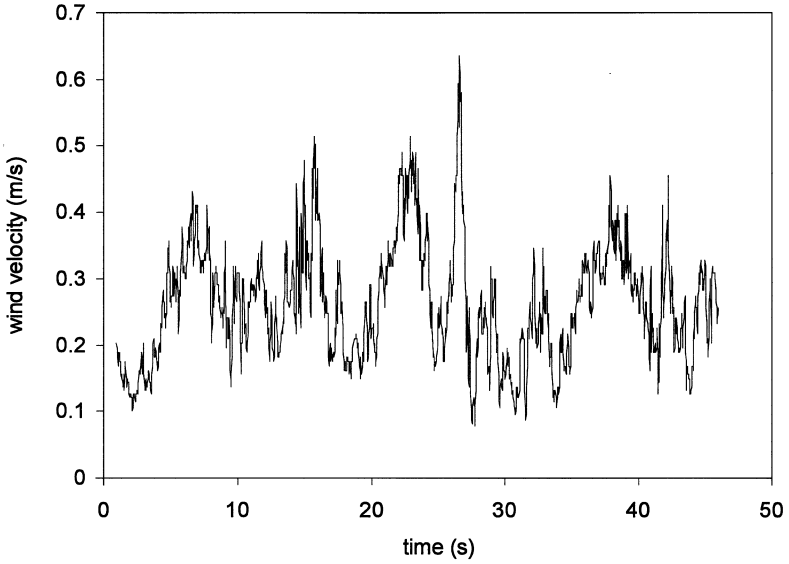

Fig. 3. Typical velocity trace used to estimate friction velocity, u_*.

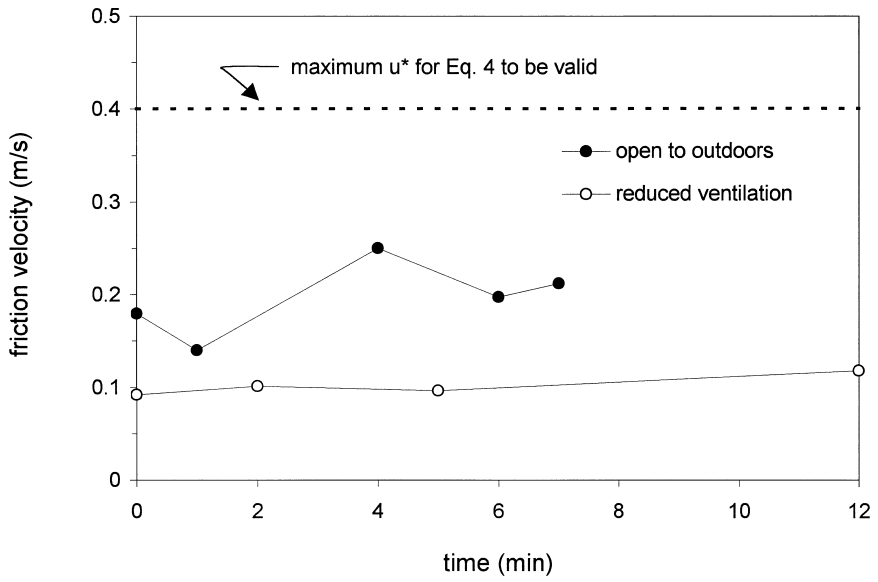

Fig. 4. Friction velocity, u_*, over time for two conditions. One series was recorded when the environment was open to the outdoors; the other was recorded when the doors were partially blocked, reducing the ventilation rate.

$u_* = 0.10$ and 0.20, respectively. Overall, the mean u and T values were $0.3\,\mathrm{m\,s^{-1}}$ and 36%, respectively.

Size distributions measured in a typical sampling event (#5) are shown in Fig. 5. The dashed line represents the average of the three passive samplers used in this event. Passive sampler error bars represent Poisson counting error, whereas the impactor error bars represent the blank detection limit.

For each sampling event, the average result of the three passive samplers was compared to that of the impactor. Fig. 6 shows passive sampler and impactor results with respect to PM2.5 and PM10 across all events. The correlation coefficients for PM2.5 and PM10 are $R^2 = 0.80$ and 0.93, respectively. Table 5 shows the percent difference between passive sampler and impactor for each sampling event, where

$$\%\ \text{difference} = \frac{\text{passive sampler result} - \text{impactor result}}{(\text{passive sampler result} + \text{impactor result})/2} \times 100\%. \tag{10}$$

The average agreement for PM2.5 and PM10 were -31 and 41%, respectively.

The precision of the three passive samplers in each sampling event is shown in Table 5. Table 5 shows that the coefficient of variation (CV) for PM2.5 was quite different for samples dominated by soda ash (events 1–3) and samples dominated by lime (events 4 and 5). The average $\mathrm{CV_{PM2.5}}$ for soda ash sampling events was 59%, while that for the lime events was 16%. The average $\mathrm{CV_{PM10}}$ across all sampling events was 20%.

4. Discussion

4.1. Turbulence

The deposition rate to the passive sampler is independent of the friction velocity only when u_* is small. Thus, the fluctuating turbulence levels of real environments have the potential to affect

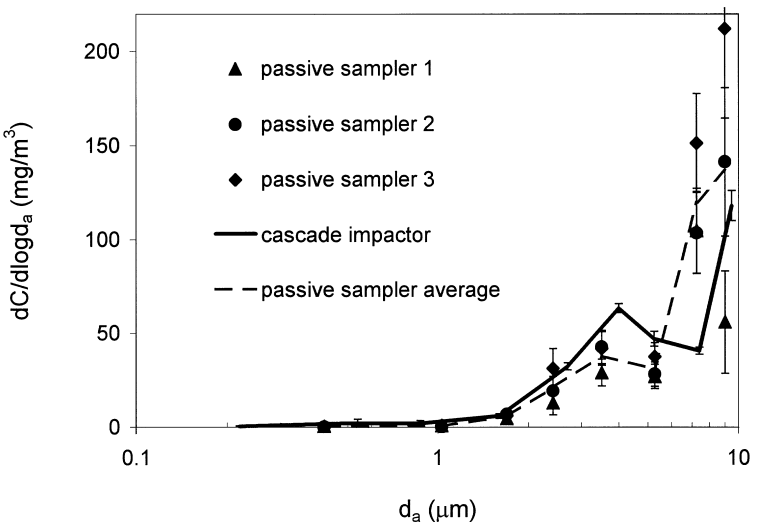

Fig. 5. Typical results: Normalized concentration, $\mathrm{d}C/\mathrm{d}\log d_a$, vs. aerodynamic particle size, d_a, for sampling event 5. The dashed line represents the average of the three passive samplers used in this event.

passive sampler results. The results presented in Fig. 4 show that changes in ventilation did produce significant changes in the mean friction velocity ($p = 0.003$). However, all measured friction velocities were less than $0.4\,\mathrm{m\,s^{-1}}$, and thus in the range required for the simplified expression of Eq. (4). Because these tests were conducted in a well-ventilated environment, the simplified expression should be valid in the many occupational, home, and indoor environments that have similar or calmer air flows. Wind speeds measured by Baldwin and Maynard (1998) in 55 diverse workplace areas support this claim. Using omnidirectional anemometers, these investigators found that 85% of measured velocities were less than $0.3\,\mathrm{m\,s^{-1}}$. In addition, their measured turbulence intensities agreed with office and home measurements made by several previous investigators, who generally found $T \cong 30$–35%. Thus, these environments all possessed turbulence levels that were equal to or less than the levels measured in this work.

An important limitation of the field apparatus used to measure turbulence is that its sampling rate was only 50 Hz, significantly lower than the several MHz resolution of a typical laboratory apparatus. Nevertheless, the lower sampling rate was judged to be adequate for estimating friction velocities. Theory and data presented by Schlichting (1979) show that the magnitude of velocity fluctuations falls off rapidly with increasing frequency, n. Following Schlichting, T is approximately a function of $n^{-5/3}$. Then, assuming an arbitrary lower limit of 2.5 Hz, measurement of velocities at 50 Hz would capture about 90% of the integrated fluctuations one would measure at 1 kHz. Because T actually decreases even more rapidly with frequency for large n, these measurements should have captured greater than 90% of the fluctuating component.

Because the measured velocities were relatively low, a second concern must be addressed. At velocities below a certain threshold, natural convection induced by the heated anemometer sensor can influence heat transfer in the vicinity of the sensor, resulting in measurement error. For ambient and sensor temperatures of 21 and 247°C, respectively, this threshold is equal to $0.05\,\mathrm{m\,s^{-1}}$ (Hinze,

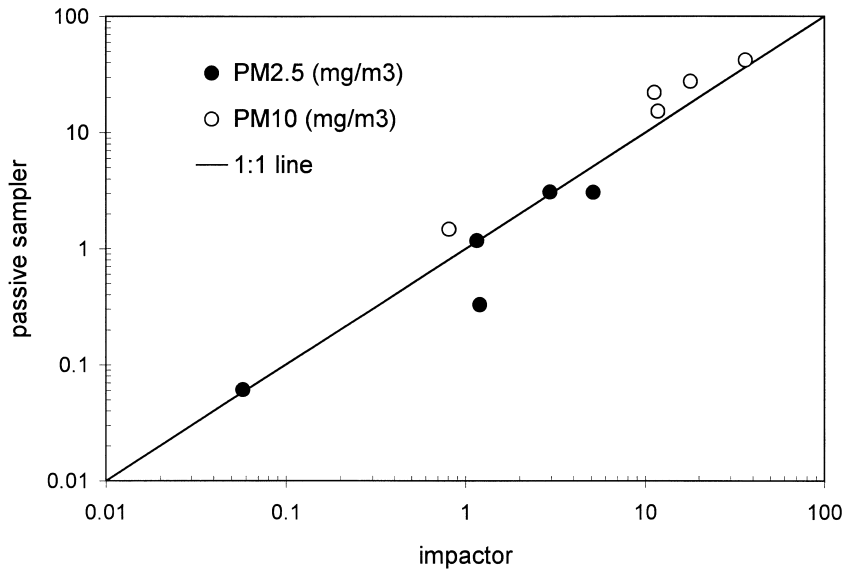

Fig. 6. PM2.5 and PM10 as measured by the passive sampler and impactor.

1975). Because 90% of the points in even the lowest-velocity trace were $>0.1\,m\,s^{-1}$, these buoyancy effects were assumed to be unimportant here.

4.2. Agreement with impactor

Fig. 6 shows that correlation between passive sampler and impactor results was good for both PM2.5 and PM10. The PM2.5 results had slightly more scatter about the 1 : 1 line, probably due to imprecision of the passive samplers (see next section).

The discrepancies found between passive sampler and impactor PM2.5 were of a different nature than those found for PM10. Fig. 7 shows the percent difference between the two sampler types' size distributions as a function of aerodynamic diameter, across all sampling events. Size distributions were compared at the impactor size bin midpoints, which required interpolation of the passive size distributions. This plot shows that disagreement for fine particles falls randomly about zero for the five sampling events. Disagreement for the coarsest particles, however, shows a similar pattern for all events, with the passive samplers recording higher concentrations than the impactors.

These observations suggest that PM2.5 discrepancies were due to random errors associated with low PM2.5 sample mass. For both sampler types, the amount of sample collected in the lowest size bins was usually on the order of the blank values.

The systematic trend in PM10 discrepancies suggests that physical mechanisms were responsible, and several possibilities exist. For one, all sampled particles showed a high degree of agglomeration (Figs. 8a and b), and thus may have had shapes and effective densities that were different from the literature values used for the passive sampler calculations. Also, local wind gradients could have caused aerosol concentrations to be different in the air spaces above the two sampler types, which were typically located about 20 cm apart.

A more likely source of discrepancy is the hygroscopicity of the soda ash that dominated 3 out of the 5 sampling events (Table 3). Evidence of water evaporation in events 2 and 3 included unstable impactor weights immediately after sampling and reduced masses when they were weighed again 24 h later. Because the impactor from event 1 sampled a much smaller mass of soda ash, the evaporated mass was difficult to detect. Loss of water mass to evaporation affects the two sampler

Table 5
Agreement with impactor and precision for passive samplers in each sampling event

Sampling event	% difference		CV (%)	
	PM2.5	PM10	PM2.5	PM10
1[a]	4.7	58	54	28
2[a]	−110	25	83	9.7
3[a]	1.1	65	40	5.2
4[b]	3.9	42	4.9	29
5[b]	−51	14	28	31

[a]Samples dominated by hygroscopic soda ash.
[b]Samples dominated by non-hygroscopic lime.

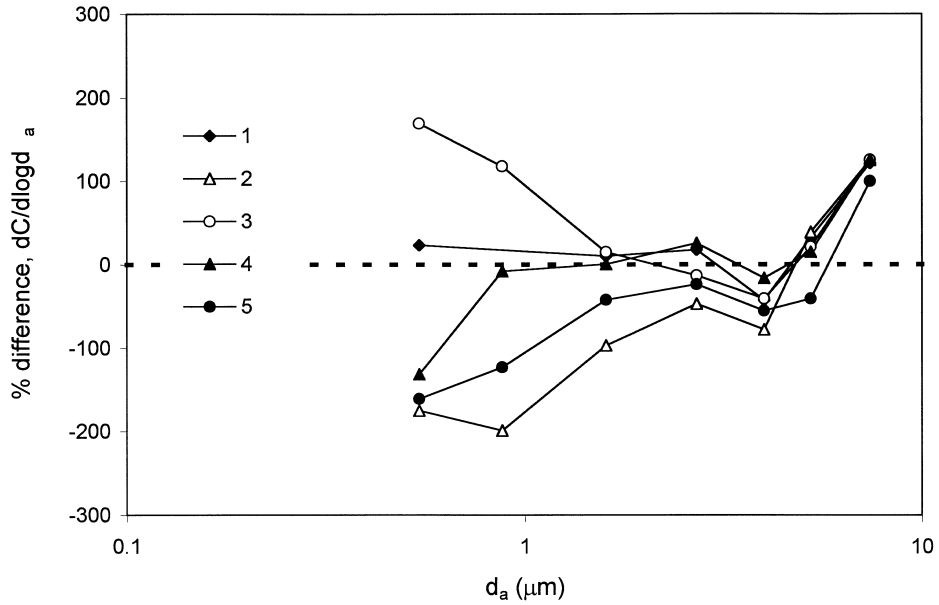

Fig. 7. Percent difference between passive sampler and impactor size distributions ($dC/d\log d_a$, vs. d_a) for all five sampling events.

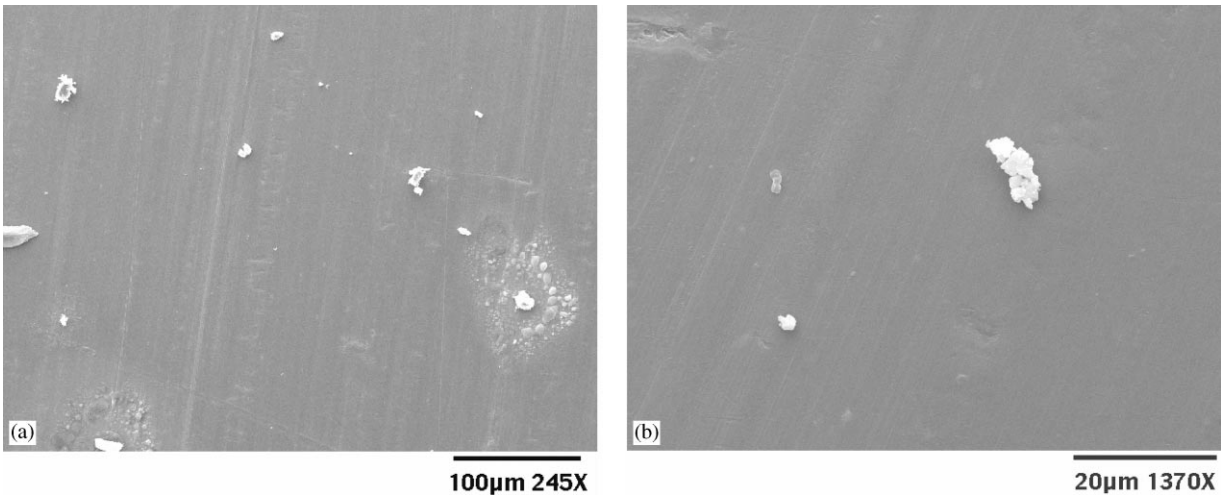

Fig. 8. SEM images from passive sampler analyses showing (a) the residue caused by evaporation of hygroscopic soda ash particles and (b) the comparatively "clean" shapes of non-hygroscopic lime particles.

types differently. For the impactor, evaporation results in a size distribution that is shifted downwards by an amount related to the water fraction of the particles. For the passive sampler, evaporation leads to underestimated particle sizes and overestimated shape factors and densities, which in turn lead to underestimated particle fluxes and deposition velocities. Assuming

equilibrium hygroscopic growth at the observed RH's, theoretical calculations show that the F and v_{dep} errors are of approximately equal sign and magnitude. As a result, the concentration for each size bin is not affected (Eq. (1)). Underestimation of the bins' nominal particle sizes, however, shifts the measured size distribution to the left. Because the shapes of the size distributions tended to have a positive slope in the coarse particle regime, the combination of these two shifts should result in passive sampler PM10 measurements that are larger than their corresponding impactor values. This outcome is consistent with what was observed.

Another likely source of discrepancy is particle bounce in the impactor. The coarse, high-concentration aerosols sampled here are likely to have bounced, despite the coated substrates used in these experiments, resulting in either deposition on the smaller stages or removal by the impactor or jet walls. This phenomenon should also cause passive sampler PM10 measurements to be larger than their corresponding impactor values, as was observed.

In light of the fact that two very different sampler types were compared in a non-laboratory setting, the correlations between passive sampler and impactor results reported here should probably be interpreted as reasonable agreement.

4.3. Precision

The soda ash- and lime-dominated passive samples exhibited very different $CV_{PM2.5}$ values, 59 and 16%, respectively. The higher $CV_{PM2.5}$ for soda ash samples is probably due to a combination of low fine-particle counts and hygroscopicity. Many of the SEM images from the passive sampler analyses from events 2 and 3 (and to a lesser extent, event 1) showed particles with "halos" of small residue particles surrounding larger cores (Fig. 8a). Others showed small, flattened shapes which were difficult to distinguish from the background. These phenomena suggest that water evaporated from these particles when the samplers were placed under the vacuum of the SEM. The residue presumably did not exist in the air, and was not considered to represent distinct particles. Because the residue was judged to have negligible mass compared to its "parent" particle cores, no effort was made to correct for the lost mass. Similarly, the flattened shapes were impossible to size accurately, and were disregarded. These decisions were unavoidably subjective, and if some of the residue and flat shapes were inadvertently counted as particles, highly variable counting and sizing of these particles would result. Because very few fine particles were present in these samples otherwise, this variability could approach the magnitude of the total PM2.5 measured. The between-sampler variability was enhanced by particle core shapes that were not always the same for samples from the same event. Because samples could not always be analyzed on the same day, some particles re-acquired water while in storage and then recrystallized in different shapes. In the future, this latter source of variability can be avoided by controlling the RH at which samples are stored. In contrast, samples dominated by the non-hygroscopic lime aerosols exhibited particles with well-defined shapes and no residue (Fig. 8b). The resulting $CV_{PM2.5}$ was much lower, even though these samples also had very low fine particle counts.

Precision was generally better for PM10 than it was for PM2.5, most likely because of many more counts, and thus better counting statistics (Table 4). Samples from events 2 and 3 recorded substantially more PM10 counts and showed the best PM10 precision. The average CV_{PM10} of 20% is slightly higher than the EPA's stated objective of 15% precision for FRM PM2.5

samplers (US Environmental Protection Agency, 1996). On the other hand, the average CV_{PM10} is much lower than 50%, the precision objective suggested by Rappaport (1994) for samplers that can be deployed easily in large numbers. Thus, the passive aerosol sampler's precision should be more than adequate for large-scale field measurements, in which concentrations at different locations within a given outdoor, indoor, or occupational environment can vary over several orders of magnitude.

5. Conclusions

The passive aerosol sampler was tested in a fairly well-ventilated occupational environment. Measured friction velocities were less than $0.4\,m\,s^{-1}$, a range in which the passive sampler's deposition model does not depend on turbulence. This result is consistent with the hypothesis that wind-speed data are not needed in most occupational and indoor environments.

Passive sampler results correlated well with those of the eight-stage cascade impactors, with $R^2 = 0.80$ and 0.93 for PM2.5 and PM10, respectively. Average disagreement between the sampler types was -31 and 41% for PM2.5 and PM10, respectively. The discrepancies in PM2.5 were likely due to errors arising from the extremely low mass of fine particles collected. The discrepancies for PM10 were probably due to the hygroscopicity of 3 of the 5 samples, as well as particle bounce in the impactors.

Water loss in the hygroscopic samples also created ill-defined particle boundaries, which led to imprecision in passive sampler PM2.5. The average $CV_{PM2.5}$ for the hygroscopic samples averaged 59%, while that for the non-hygroscopic samples was much lower, 16%. The average CV_{PM10} for all samples was 20%. These results suggest that the passive sampler will exhibit some imprecision when measuring aerosols with large hygroscopic fractions. On the other hand, the results suggest that the passive sampler should exhibit good precision when measuring non-volatile particles in the field. In addition, the sensitivity of the passive sampler to hygroscopic losses should be reduced substantially if analysis is performed under ambient pressures, e.g. with an environmental SEM.

Thus far, the passive sampler has been tested only with high aerosol concentrations over durations of a few hours. However, the sampler also has utility for measuring chronic aerosol exposures, i.e. lower concentrations with sampling times on the order of days. Future work will include testing of the sampler with other concentration and time scales, implementation of the passive aerosol sampler as a personal sampler, and improvements to the analysis procedure.

Acknowledgements

The authors wish to thank Maryanne Boundy for her assistance during the field tests, as well as the National Institute for Occupational Safety and Health (1 R03 OHO3774-01) and US Environmental Protection Agency (U-915321-01-0) for supporting this work.

References

Baldwin, P. E., & Maynard, A. D. (1998). A survey of wind speeds in indoor workplaces. *Annals of Occupational Hygiene*, *42*, 303–313.

Brown, R. C., Hemingway, M. A., Wake, D., & Thompson, J. (1995). Field trials of an electret-based passive dust sampler in metal-processing industries. *Annals of Occupational Hygiene*, *39*, 603–622.

CRC Handbook of Chemistry and Physics (1997). (77th ed.) Boca Raton, FL: CRC Press.
Davies, C. N. (1979). Particle-fluid interaction. *Journal of Aerosol Science*, *10*, 477–513.
Hinze, J. (1975). *Turbulence* (2nd ed.) (pp. 90–91). New York: McGraw-Hill.
Hughmark, G. (1977). Turbulence properties in the core of pipe flow. *Industrial and Engineering Chemistry, Fundamentals*, *16*, 307–308.
McCrone, W. C., & Delly, J. G. (1973a). *The particle atlas, vol. 2* (2nd ed.). Ann Arbor, MI: Ann Arbor Science.
McCrone, W. C., & Delly, J. G. (1973b). *The particle atlas, vol. 3* (2nd ed.). Ann Arbor, MI: Ann Arbor Science.
Noll, K. E., Fang, K. Y. P., & Watkins, L. A. (1988). Characterization of the deposition of particles from the atmosphere to a flat plate. *Atmospheric Environment*, *22*, 1461–1468.
Rappaport, S. M. (1994). Interpreting levels of exposures to chemical agents. In R.L. Harris, L.J. Cralley, & L.V. Cralley, *Patty's industrial hygiene and toxicology*, *vol. 3*, *Part A* (3rd ed.) (pp. 349–403). New York: Wiley.
Schlichting, H. (1979). *Boundary-layer theory* (7th ed.) (pp. 457, 475). New York: McGraw-Hill.
Schneider, T., Bohgard, M., & Gudmundsson, A. (1994). A semiempirical model for particle deposition onto facial skin and eyes. Role of air currents and electric fields. *Journal of Aerosol Science*, *25*, 583–593.
Thorpe, A., Hemingway, M. A., & Brown, R. (1999). Monitoring of urban particulate using an electret-based sampler. *Applied Occupational Environment Hygiene*, *14*, 750–758.
Turner, J., & Hering, S. (1987). Greased and oiled substrates as bounce-free impaction surfaces. *Journal of Aerosol Science*, *18*, 215–224.
US Environmental Protection Agency (1996). Proposed requirements for designation of reference and equivalent methods for PM2.5 and ambient air quality surveillance for particulate matter. *Federal Register*, *61*(241) 65785.
Wagner, J., & Leith, D. (2000a). Passive aerosol sampler. I: Principle of operation. *Aerosol Science and Technology*, in press.
Wagner, J., & Leith, D. (2000b). Passive aerosol sampler. II: Wind tunnel experiments. *Aerosol Science and Technology*, in press.
Wood, N. B. (1981). A simple method for the calculation of turbulent deposition to smooth and rough surfaces. *Journal of Aerosol Science*, *12*, 275–290.